

Evaluating Transparent Reasoning in Large Language Models for Accountable Critical Tasks

Junhao Chen*, Bowen Wang, *Member, IEEE*, Jiuyang Chang*, and Yuta Nakashima, *Member, IEEE*,

Abstract—This paper introduces REACT, a benchmark designed to rigorously evaluate the reasoning capabilities of large language models (LLMs) within accountable, high-stakes decision-making tasks in medical and legal domains. Unlike traditional benchmarks primarily focused on prediction accuracy, REACT emphasizes transparent and interpretable reasoning, requiring models to align their logic closely with expert-derived procedures. To assess whether LLM reasoning aligns closely with human experts, we annotated 511 clinical cases from the medical domain and 86 legal cases from the legal domain, each enriched with detailed expert-extracted rationales and evidence supporting each step of the reasoning process. These annotations were guided by carefully constructed reasoning graphs, which explicitly encode domain-specific inference structures and decision criteria derived by domain experts. These reasoning graphs serve not only as standards for expert annotation but also as structured guidelines enabling models to reason transparently and step-by-step. To address the scalability challenges of manual annotation, we further developed a semi-automatic annotation pipeline leveraging expert-defined reasoning graph templates to efficiently generate new graphs, exploring the potential to extend our approach into additional critical domains. Experimental results demonstrate that reasoning graphs substantially enhance the interpretability and accuracy of LLM reasoning compared to traditional baselines, although significant gaps remain relative to expert-level reasoning performance.

Index Terms—Reasoning Graph, Large Language Model, Explainable AI, Semi-automatic Annotation, Diagnostic Reasoning, Judicial Reasoning

I. INTRODUCTION

Through pre-training and instruction tuning, Large Language Models (LLMs) have acquired extensive world knowledge and strong capabilities in following human instructions to output corresponding knowledge [1]–[4]. This end-to-end generation capability significantly lowers the barrier to their use, resulting in widespread adoption across various domains, such as question answering [5], [6], multi-turn dialogue [7], [8], and code generation [9], [10]. In high-stakes fields like medicine and law, where incorrect decisions can lead to severe

This work was supported by World Premier International Research Center Initiative (WPI), MEXT, Japan. This work is also supported by JSPS KAKENHI 24K20795 and JST ACT-X Grant Number JPMJAX24C8.

Junhao Chen is an intern student at D3 Center, The University of Osaka (e-mail: junhao@ids.osaka-u.ac.jp). Bowen Wang is with Premium Research Institute for Human Metaverse Medicine (WPI-PRIME) and D3 Center, The University of Osaka, 2-2 Yamadaoka, Suita, Osaka 565-0871 (e-mail: wang@ids.osaka-u.ac.jp). Jiuyang Chang is with Department of Cardiology, The First Affiliated Hospital of Dalian Medical University (e-mail: changjiuyang@firsthosp-dmu.com). Yuta Nakashima is with SANKEN, department of Intelligent Media, The University of Osaka (e-mail: n-yuta@im.sanken.osaka-u.ac.jp).

* Junhao Chen and Jiuyang Chang are with equal contributions.

Corresponding author: wang@ids.osaka-u.ac.jp

consequences such as delayed treatment or misjudged criminal liability, stricter requirements are imposed for interpretability, reasoning traceability, and accountability [11], [12]. Therefore, in these critical applications, LLMs must not only generate accurate answers but also demonstrate clear, traceable reasoning and transparent logic to meet the stringent demands for interpretability and accountability.

While existing benchmarks in medicine and law primarily evaluate LLMs based on the correctness of their final predictions, they often pay little attention to whether the reasoning process is transparent or aligned with domain-expert logic [13]–[16]. Natural Language Inference (NLI) tasks offer a closer approximation to reasoning process evaluation, as they explicitly present premises and hypotheses, testing the model’s ability to infer conclusions [17], [18]. However, real-world scenarios in high-stakes domains rarely present well-structured premises and hypotheses. Instead, models must first identify and extract relevant evidence from lengthy case records, such as clinical notes or legal rulings, before reasoning toward a compliant and justified conclusion. As such, realistic evaluation in these domains requires end-to-end assessments of their ability to perform evidence extraction, logical reasoning, and attribution reasoning. Existing benchmarks are limited in their ability to capture the complexity and rigor of reasoning required in these settings.

To bridge this gap, we introduce REACT, a benchmark designed to evaluate whether LLMs can reach accurate conclusions and expert domain-aligned reasoning when grounded in real-world, long-form case records. Our benchmark primarily focuses on the medical domain, where we curate 511 clinical notes spanning 25 disease categories from the MIMIC-IV database [19], annotated by medical experts with both key evidence and full clinical reasoning chains. To test the generalizability of the LLMs and different baseline settings, we additionally include a smaller set of 86 legal case rulings from the China Judgments Online¹. These cases, drawn from China’s civil law system rather than common law and covering eight types of criminal offenses, are annotated by legal professionals to capture the statutory reasoning processes. This setup allows us to conduct fine-grained evaluations of both predictive accuracy and reasoning quality. To facilitate annotation consistency and support LLM reasoning, we construct reasoning graphs based on medical diagnostic guidelines and legal provisions. These graphs explicitly encode multi-step inference structures and domain knowledge required in the reasoning process, serving both as scaffolds for annotation and

¹China Judgments Online: <https://wenshu.court.gov.cn>

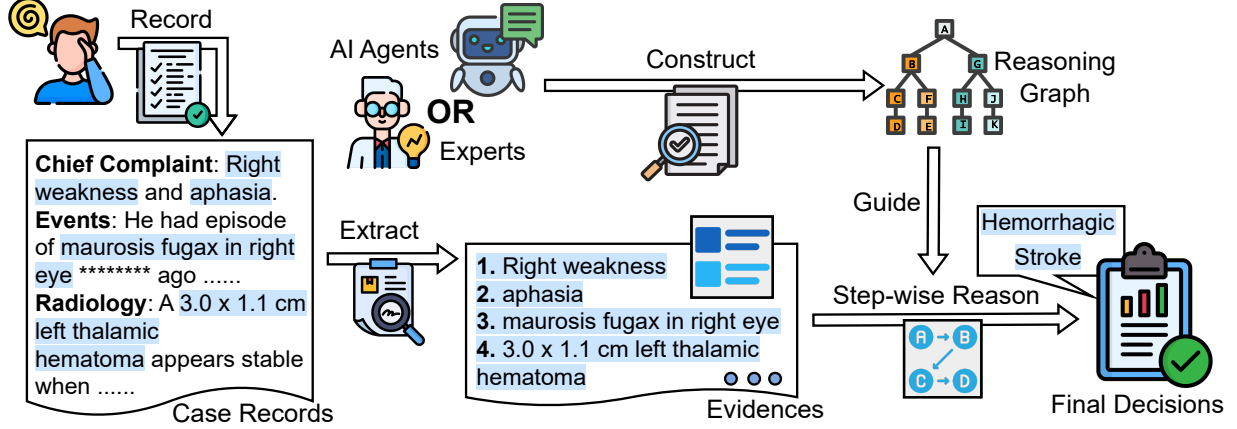


Fig. 1. A step-wise reasoning pipeline from case records to final decisions in the REACT benchmark.

guides for LLMs to improve interpretability and accuracy. The overall pipeline of reasoning from raw case records to final decisions, guided by these graphs, is illustrated in Figure 1.

Constructing these graphs manually requires substantial time and domain expertise, making it difficult to scale. Therefore, we propose a workflow-based AI agent that automatically generates reasoning graphs based on the graph backbones designed by the experts. Experimental results demonstrate that the AI agent’s outputs align well with expert annotations, facilitating the efficient expansion of annotated reasoning resources with minimal human effort. To highlight the challenges posed by our dataset, we develop an AI-agent baseline that leverages the reasoning graphs to sequentially infer the conclusion. Experiments reveal that these graphs, whether created by experts or AI agents, significantly improve both the accuracy and interpretability of LLMs over standard baselines such as RAG [20], Graph RAG [21], and zero-shot prompting. Nonetheless, even the strongest current LLMs struggle to match expert-level reasoning, underscoring the difficulty and significance of this benchmark.

This work is an extension of our NeurIPS 2024 conference paper [22], providing broader validation and deeper analysis. Specifically: (1) We develop a semi-supervised annotation pipeline to explore whether our reasoning approach can be extended to additional domains with minimal annotation. (2) We introduce a legal-domain dataset for cross-domain evaluation, demonstrating the generalizability of our conclusions and reasoning approach. (3) We include free-form baselines, such as Retrieval-Augmented Generation (RAG) and Graph-based RAG, for comparison, underscoring the continued importance of structured guidance. Together, these contributions provide new insights into model behavior, robustness under varied conditions, and domain transfer characteristics, informing future work directions.

Contribution We present REACT, a benchmark for reasoning in accountable critical tasks across the medical and legal domains. The task requires models to extract relevant evidence from long-form case records and align their reasoning process with domain experts. To support this, we present the Reasoning Dataset for High-Stake Domains, built around multi-evidence reasoning graphs. These graphs go beyond

TABLE I
COMPARISON OF EXISTING DATASETS FOR MEDICAL AND LEGAL REASONING TASKS AND OURS. “T”, “W”, AND “C” REFER TO TOKENS, WORDS, AND CHINESE CHARACTERS, RESPECTIVELY.

Dataset	Task	Data Source	Length	Explanation	# Cases
Medical Datasets					
MedMCQA [13]	QA	Examination	9.93 t	Plain Text	194,000
ExplainCPE [23]	QA	Examination	37.79 w	Plain Text	7,000
JAMA Challenge [24]	QA	Clinical Cases	371 w	Plain Text	1,524
Medbullets [24]	QA	Online Questions	163 w	Plain Text	308
N2N2 [25]	Sum	Clinical Notes	785.46 t	Evidences	768
NLI4CT [14]	NLI	Clinical Trial Reports	10–35 t	Multi-hop	2,400
NEJM CPC [26]	CD	Clinical Cases	–	Plain Text	2,525
REACT (Ours)	CD	Clinical Notes	1074.6 t	Entailment Tree	511
Legal Datasets					
IEC-QA [15]	QA	Examination	47.01 c	Plain Text	26,365
cLegal-QA [27]	QA	Examination	50 c	Plain Text	14,000
LegalQA [28]	QA	Online Questions	150 w	Plain Text	2,200
EQUALS [29]	QA	Online Questions	98 c	Plain Text	6,914
CVG [30]	Sum	Legal Case	219.9 t	Plain Text	222,482
PILOT [31]	JP	Legal Case	–	Legal Provisions	14,138
CAIL2018 [16]	JP	Legal Case	–	Legal Provisions	2,676,075
LEO [32]	NLI	Legal Case	–	Entailment Tree	453
REACT (Ours)	JP	Legal Case	5058.8 t	Entailment Tree	86

traditional NLI or single-step inference tasks, providing a more comprehensive and realistic benchmark for evaluating LLMs’ capabilities in complex scenarios. By making the model’s reasoning transparent and verifiable, even when it lacks full domain knowledge, our benchmark promotes reliability and interpretability in High-Stake environments. Furthermore, our automated reasoning graph AI agent lays the groundwork for scaling high-quality annotated resources, ultimately enabling broader deployment of decision-support systems in medicine and law.

II. RELATED WORKS

Natural language explanation. Recent advancements in NLP have led to significant achievements [33]. However, existing models often lack explainability, posing potential risks [34], [35]. Numerous efforts have been made to address this challenge. One effective approach is to provide a human-understandable *plain text* explanation alongside the model’s output [36], [37]. Another strategy involves identifying *evidence* within the input that serves as a rationale for the model’s decisions, aligning with human reasoning [38]. Expanding on this concept, [39] introduces chain-structured explanations, given that a diagnosis can demand multi-hop reasoning. This idea is further refined by ProofWriter [40] through a proof

stage for explanations, and by [41] through retrieval from a corpus. [42] proposes the *entailment tree*, offering more detailed explanations and facilitating inspection of the model’s reasoning. More recently, [43] employed cumulative reasoning to tap into the potential of LLMs to provide explanation via a *directed acyclic graph*. Although substantial progress has been made, interpreting NLP tasks in medical domains remains an ongoing challenge [44].

Benchmarks of interpretability in the medical domain

Several datasets are designed to assess a model’s reasoning together with its interpretability in medical NLP (Table I). MedMCQA [13] and other medical QA datasets [23], [24] provide plain text as explanations for QA tasks. NLI4CT [14] uses clinical trial reports, focusing on NLI supported by multi-hop reasoning. N2N2 [25] proposes a summarization (Sum) task for a diagnosis based on multiple pieces of evidence in the input clinical note. NEJM CPC [26] interprets clinicians’ diagnostic reasoning as plain text for reasoning clinical diagnosis (CD). DR.BENCH [45] aggregates publicly available datasets to assess the diagnostic reasoning of LLMs. Utilizing an multi-evidence entailment tree explanation, DiReCT introduces a more rigorous task to assess whether LLMs can align with doctors’ reasoning in real clinical settings.

Benchmarks of interpretability in the legal domain

Several datasets are designed to evaluate a model’s reasoning ability and interpretability in legal natural language processing tasks (Table I). The most fundamental are question-answering tasks. For example, JEC-QA [15] provides multiple-choice questions with option analyses, while cLegal-QA [27] and LegalQA [28] use long-form answers as evaluation standards. EQUALS [29] focuses on extracting answers from legal statutes based on the given questions. CVG (COURT VIEW GENeration) [30] introduces the task of “court view generation,” aiming to identify judges’ reasoning from the factual descriptions of criminal cases, assisting humans or models in making decisions. PILOT [31] and CAIL2018 [16] provide JP (judgment prediction) tasks that require models to output not only the verdict but also the corresponding legal statutes as explanations, in order to assess whether language models can reach correct decisions based on legal grounds. LEO (Legal Experience Ontology) [32] introduces a structured reasoning task that requires models to extract elements such as Factum Probandum, Evidence, and Experiences from case texts, building a tree-structured legal reasoning process. However, in this task, the model is not asked to make judgments itself, but the inferred results are from case texts.

III. A BENCHMARK FOR CASE RECORDS REASONING

This section introduces the benchmark constructed from “case records” in two high-stakes domains: medicine and law. We first describe the structure and sources of the case records used in our benchmark (Section III-A), followed by the Reasoning Graphs that encode domain-specific decision-making processes (Section III-B). The task definition, which takes a case record and an optional external knowledge source as input, is provided in Section III-D. We then outline our expert annotation process for clinical and legal cases (Sec-

tion III-C) and present the evaluation metrics used to assess model performance (Section III-E).

A. Case Records

Our benchmark is constructed from two types of high-stakes domain case records: clinical notes from the medical domain and legal rulings from the legal domain.

The clinical notes are sourced from the MIMIC-IV benchmark [19] (PhysioNet Credentialed Health Data License 1.5.0), which contains medical records for over 40,000 ICU patients. From this, we curated a subset of 511 notes covering 25 disease categories across 5 medical domains. Each note follows the SOAP format [46], consisting of four sections: *subjective*, *objective*, *assessment*, and *plan*. The subjective section includes the chief complaint, history of present illness, and other subjective experiences reported by the patient. The objective section contains structured data obtained from physical exams and laboratory tests. The assessment section provides the physician’s clinical judgment and may include a summary of the current condition. The plan section outlines the proposed treatment, including medications, recommended therapies, or further investigations.

In our task setting, each medical record $R = r$ is a snippet composed of six types of clinical data from the subjective and objective sections (i.e., $|R| = 6$): chief complaint, history of present illness, past medical history, family history, physical exam, and pertinent results.² We also identified the PDD d^* associated with R .³ The set of d^* ’s for all R ’s collectively forms \mathcal{D}^* . We manually removed any descriptions that disclose the PDD in R .

The legal rulings are sourced from publicly available criminal verdicts on the China Judgments Online. From this, we curated a subset of 86 verdicts covering 8 offense types across 4 major legal categories: crimes against life and health, crimes infringing on sexual autonomy, crimes violating reputation, privacy, and information rights, and crimes restricting personal liberty. Unlike clinical notes, these records are written in a free-form narrative by local courts without a standardized format.

In our task setting, each legal record $R = r$ is a complete case document that may contain descriptions of case facts, procedural history, evidentiary materials, and legal arguments, written in free-form narrative by various local courts. Since these rulings are not composed according to a standardized structure, each record is treated as a single unit (i.e., $|R| = 1$). Our legal experts anonymized the documents by retaining only surnames and manually redacted any language that directly reveals the final judgment outcome. Since nearly all public cases on the platform end in convictions, we revised a subset to simulate acquittals, ensuring more balanced label coverage. Each legal record is associated with a final ruling d^* , representing the court’s legal judgment (e.g., conviction or acquittal for a specific offense). The set of d^* ’s for all R ’s collectively

²We excluded data, such as review system and social history, because they are often missing in the original clinical notes and are less relevant to the diagnosis.

³All clinical notes in this benchmark are related to only one PDD, and there is no secondary discharge diagnosis.

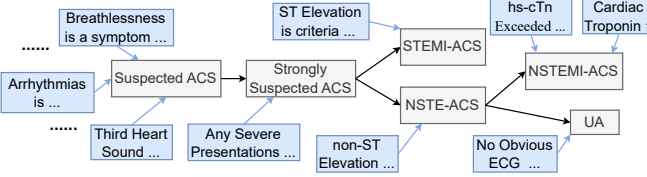


Fig. 2. A part of k_i for i being Acute Coronary Syndromes.

forms \mathcal{D}^* . As with the medical data, any content in R that may disclose d^* directly was manually removed.

B. Reasoning Graph

Existing knowledge graphs in high-risk domains, such as UMLS KG [47], are not designed to provide reasoning support. They lack structured inference paths that guide models through step-by-step reasoning and often omit critical information such as diagnostic thresholds and context-specific conditions. These components are essential in domains such as medicine and law, where decisions are complex, context-sensitive, and carry significant real-world consequences.

To address this gap, we introduce a new type of knowledge graph, which we refer to as Reasoning Graphs. Unlike conventional knowledge graphs that primarily encode static factual relations, Reasoning Graphs explicitly represent the dynamic reasoning process. The backbone of a Reasoning Graph is a procedural graph $g_i = (\mathcal{D}_i, \mathcal{F}_i)$, which captures the step-by-step progression of reasoning for a specific category i (e.g., disease or offense type). Each node in \mathcal{D}_i represents a reasoning-stage diagnosis or judgment, and each directed edge in $\mathcal{F}_i = (d, d')$ denotes a procedural transition where d' is derived from d . The procedural graph is structured as a tree rooted in an initial diagnosis or charge and branches into multiple possible final decisions (i.e., primary discharge diagnoses or verdicts), denoted as leaf nodes $\mathcal{D}_i^* \subset \mathcal{D}_i$. The complete set of procedural graphs is $\mathcal{G} = g_i$.

Building on this procedural backbone, we incorporate additional nodes and edges that represent the knowledge supporting each step. Specifically, each Reasoning Graph $\mathcal{K} = k_i$ includes domain-specific premises \mathcal{P}_i (e.g., medical or legal facts), and *supporting edges* $\mathcal{S}_i = (p, d)$ connecting a premise $p \in \mathcal{P}_i$ to a reasoning-stage node $d \in \mathcal{D}_i$. These supporting edges represent the contextual or factual requirements necessary to justify a decision at a given stage. Formally, the complete Reasoning Graph for a category i is defined as $k_i = (\mathcal{D}_i, \mathcal{P}_i, \mathcal{S}_i, \mathcal{F}_i)$, integrating both the procedural reasoning flow and the factual premises supporting it.

Figure 2 shows a partial Reasoning Graph k_i for Acute Coronary Syndromes (ACS). Blue and gray boxes represent premises and reasoning nodes, respectively; blue arrows denote supporting edges, and black arrows indicate procedural flows.

These Reasoning Graphs serve as two essential functions: (1) They serve as the gold standard for annotation, guiding experts in the precise and uniform interpretation of case records. (2) Our task also allows a model to use them to ensure the output from an LLM can be closely aligned with the reasoning processes of experts in medicine and law.

TABLE II
STATISTICS OF MEDICAL AND LEGAL CATEGORIES. “T” REFERS TO TOKENS.

Category	# Cat.	# Cases	$ \mathcal{D}_i $	$ \mathcal{D}_i^* $	$ \mathcal{O} $	Length
Medical Categories						
Cardiology	7	184	27	16	8.7	1156.6 t
Gastroenterology	4	103	11	7	4.3	1026.0 t
Neurology	5	77	17	11	11.9	1186.3 t
Pulmonology	5	92	26	17	10.7	940.7 t
Endocrinology	4	55	20	14	6.9	1063.5 t
Overall (Medical)	25	511	101	65	8.5	1074.6 t
Legal Categories						
Life & Health	4	42	12	8	16.3	6892.0 t
Sexual Autonomy	2	21	6	4	15.9	3622.3 t
Reputation/Privacy	1	11	3	2	19.7	2361.5 t
Personal Liberty	1	12	3	2	21.4	5097.0 t
Overall (Legal)	8	86	24	16	17.2	5058.8 t

C. Data Annotation

Let $d^* \in \mathcal{D}_i^*$ denote the final decision of category i associated with a case record R . For each d^* , we identify a subgraph $k_i(d^*)$ of k_i that includes all its ancestor nodes and corresponding premises in \mathcal{P}_i , and denote the set of supporting edges as $\mathcal{S}_i(d^*)$. For each supporting edge $(p, d) \in \mathcal{S}_i(d^*)$, annotators extract all observations $\{o_j\} \subset \mathcal{O}$ from R that jointly or individually support the edge, and for each o_j provide a rationalization z_j explaining why o_j supports d or corresponds to p . These annotated triplets $\{(o_j, z_j, d)\}$ collectively form the explanation set $\mathcal{E} = \{(o, z, d)\}$ for the pair (R, d^*) . For clinical records, annotations were performed by 9 physicians and verified by 3 senior medical experts. If certain expected observations were missing from R (e.g., due to omitted tests), annotators were instructed to add plausible content based on clinical knowledge to ensure a complete reasoning path.⁴ For legal records, the same procedure was applied: given a legal case R and a final judgment d^* , annotators extracted observation spans and provided rationales aligned with the legal reasoning graph k_i . These annotations were performed by master’s students in law and reviewed multiple times to ensure both accuracy and consistency.

Tables II summarize the statistics of the benchmark across medical and legal domains, respectively. The columns “# Cat.” and “# Cases” indicate the number of subcategories and annotated case records per domain. $|\mathcal{D}_i|$ and $|\mathcal{D}_i^*|$ denote the total number of intermediate and final decisions, aggregated over all categories. $|\mathcal{O}|$ represents the average number of annotated observations per case, and “Length” refers to the average token count of each case record R .

D. Task Definition

We propose a flexible reasoning task that allows optional support through various types of external knowledge. Given a case record R , the objective is to predict the final decision d^* and generate an explanation \mathcal{E} that reconstructs the reasoning

⁴All annotations strictly follow the procedural flow in k_i , and each observation is only related to one diagnostic node. Refer to the amended data points in the supplementary for details.

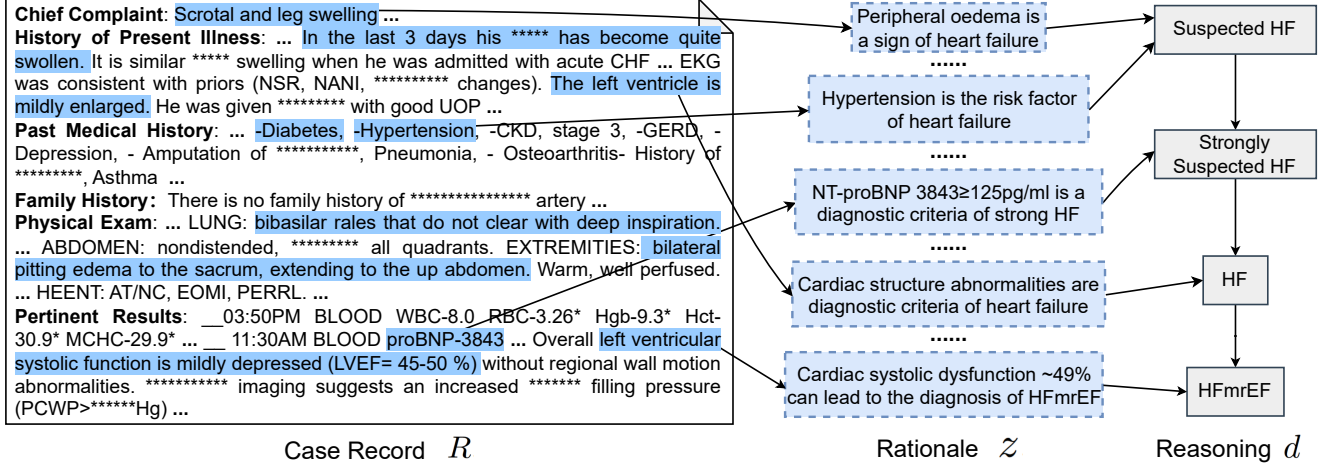


Fig. 3. An annotation sample of Heart Failure (HF). The left part is the clinical note alongside extracted observations by a doctor. The middle part outlines the steps of the rationale for the premise corresponding to each diagnostic node shown in the right part.

path from R to d^* . Letting M denote a model, the prediction is defined as:

$$\hat{d}^*, \hat{\mathcal{E}} = M(R, \mathcal{G}/\mathcal{K}/\mathcal{T}/\emptyset),$$

where $\hat{d}^* \in \cup_i \mathcal{D}_i^*$ is the predicted decision and $\hat{\mathcal{E}}$ is the generated explanation. The model may optionally receive external input in four forms: (1) procedural knowledge graphs \mathcal{G} derived from structured domain guidelines, (2) extended knowledge graphs \mathcal{K} , which augment \mathcal{G} with broader domain-level facts and auxiliary premises, (3) free-form reference text \mathcal{T} such as excerpts from textbooks or public resources, or (4) no external input at all (\emptyset).

When supplied with \mathcal{G} , the model can follow structured reasoning procedures aligned with expert decision-making protocols. When \mathcal{K} is used, additional contextual knowledge can be incorporated to support inference beyond procedural flows. \mathcal{T} offers greater flexibility in the form of a textual background without requiring a formal graph structure. The no-input setting (\emptyset) evaluates the model's internalized knowledge and reasoning capability.

All predictions follow a step-wise reasoning process. Rather than jointly producing the decision and explanation, the model is expected to output intermediate reasoning steps by the baseline strategies described in the following sections.

E. Evaluation Metrics

We designed three metrics to quantify the predictive performance over our benchmark.

(1) *Accuracy of reasoning* evaluates whether the model predicts the correct final decision d^* for a given case. We report two metrics: $Acc^{dec} = 1$ if the predicted decision \hat{d}^* exactly matches the ground truth d^* , and $Acc^{cat} = 1$ if \hat{d}^* belongs to the same domain category i as d^* (i.e., $\hat{d}^* \in \mathcal{D}_i^*$ where $d^* \in \mathcal{D}_i^*$). The former captures fine-grained correctness, while the latter reflects whether the model is reasoning within the correct semantic or procedural scope.

(2) *Completeness of observations* Obs^{comp} evaluates whether a model extracts all and only necessary observations for the

prediction. Let \mathcal{O} and $\hat{\mathcal{O}}$ denote the sets of observations in \mathcal{E} and $\hat{\mathcal{E}}$, respectively. The metric is defined as $Obs^{comp} = |\mathcal{O} \cap \hat{\mathcal{O}}|/|\mathcal{O} \cup \hat{\mathcal{O}}|$, where the numerator is the number of observations that are common in both \mathcal{O} and $\hat{\mathcal{O}}$.⁵ This metric simultaneously evaluates the correctness of each observation and the coverage. To supplement it, we also report the precision Obs^{pre} and recall Obs^{rec} , given by $Obs^{pre} = |\mathcal{O} \cap \hat{\mathcal{O}}|/|\hat{\mathcal{O}}|$ and $Obs^{rec} = |\mathcal{O} \cap \hat{\mathcal{O}}|/|\mathcal{O}|$.

(3) *Faithfulness of explanations* evaluates if the reasoning flow toward the final decision of category is fully supported by observations with faithful rationalizations. This involves establishing a one-to-one correspondence between deductions in the prediction and the ground truth. We use the correspondences established for computing Obs^{comp} . Let $o \in \mathcal{O}$ and $\hat{o} \in \hat{\mathcal{O}}$ denote corresponding observations. This correspondence is considered successful if z and \hat{z} as well as d and \hat{d} associated with o and \hat{o} matches. Let $m(\mathcal{E}, \hat{\mathcal{E}})$ denote the number of successful matches. We use the ratio of $m(\mathcal{E}, \hat{\mathcal{E}})$ to $|\mathcal{O} \cap \hat{\mathcal{O}}|$ and $|\mathcal{O} \cup \hat{\mathcal{O}}|$ as evaluation metrics Exp^{com} and Exp^{all} , respectively, to see failures come from observations or explanations and reasoning.

IV. SEMI-AUTOMATIC ANNOTATION

To alleviate the high cost of manually constructing reasoning graphs \mathcal{K} in complex domains such as medicine and law, we propose a semi-automatic annotation framework that leverages expert-defined procedural backbones \mathcal{G} to automatically induce factual reasoning graphs \mathcal{K}' . The workflow proceeds in three stages: (1) extracting atomic knowledge from text, (2) filtering and consolidating redundant information, and (3) injecting the resulting knowledge into \mathcal{G} to produce \mathcal{K}' , a lexicalized reasoning graph aligned with domain logic. This automatically generated \mathcal{K}' can be used as a starting point for expert annotation or evaluation. To assess the quality of these graphs, we introduce metrics that measure their alignment with expert-annotated counterparts \mathcal{K} .

⁵We find the common observations with an LLM (refer to the supplementary material for more detail).

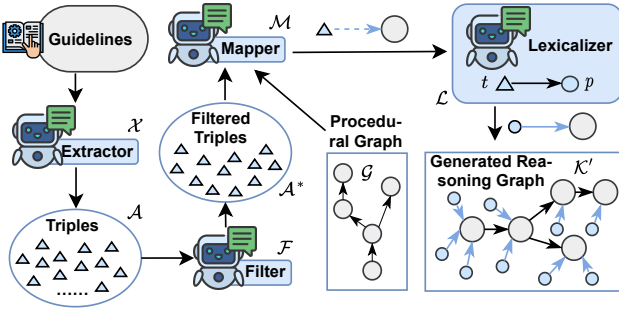


Fig. 4. The semi-automatic annotation workflow in REACT. This figure illustrates the process of transforming raw domain knowledge into structured reasoning graphs. The workflow includes extracting atomic knowledge triples, filtering redundant or irrelevant content, mapping filtered knowledge to procedural graph structures, and converting them into lexicalized premises. The resulting reasoning graphs support efficient annotation and model interpretability in high-stakes domains.

A. Knowledge Extraction

We begin by extracting atomic knowledge units in the form of triples $(h, r, t) \in \mathcal{A}$, where h and t denote entities and r represents their relation. The extraction is handled by a domain-adapted extractor module \mathcal{X} , which takes textual segments as input and outputs triples expressing atomic knowledge.

In the medical domain, clinical guidelines are segmented into manageable units using SentenceSplitter from llama_index⁶. Each paragraph is processed by \mathcal{X} to produce diagnostic triples. Numeric values are preserved in their original form, and mathematical symbols are translated into natural language (e.g., “ \geq ” becomes “greater than or equal to”) to ensure each triple reflects a single, interpretable diagnostic criterion. In contrast to the medical domain, where structured clinical guidelines are readily available, the legal domain in China lacks explicit written judgment guidelines. To address this, we incorporate the “Three-Tier Theory” of Chinese criminal jurisprudence [48] as a conceptual framework. Large language models are prompted with both this theory and the statutory provisions relevant to a particular offense to generate structured judgment guidelines. From these outputs, the extractor module \mathcal{X} identifies and extracts detailed triples that capture the elements of offense, unlawfulness, and culpability.

B. Redundant Information Filtering

To reduce semantic redundancy and improve graph quality, all triples in \mathcal{A} are encoded using a Sentence-Transformer model ϕ . Each entity h, t and relation r is embedded as $\phi(h)$, $\phi(r)$, and $\phi(t)$ respectively. If both entities in two triples exceed a similarity threshold of 0.99 and the relations exceed 0.95, the two triples are merged into one canonical form.

In medicine, a domain-specific filter module \mathcal{F}_{med} retains only those triples directly associated with risk factors, symptoms, clinical signs, or diagnostic criteria. Triples concerning treatments or unrelated clinical details are discarded. In law, a legal filter module \mathcal{F}_{law} applies heuristic rules to merge semantically equivalent expressions of legal elements, such

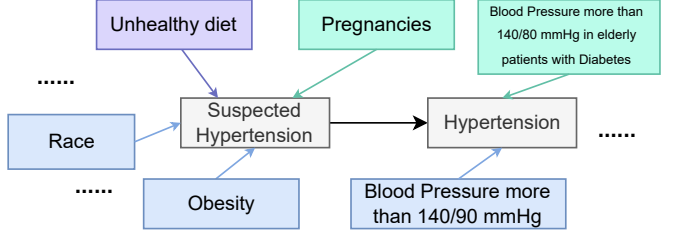


Fig. 5. Graph segment from \mathcal{K}' for the Hypertension case. Blue nodes denote generated knowledge that aligns with the expert-defined template \mathcal{K} ; purple nodes indicate missing (unmatched) expert knowledge; cyan nodes represent additional content not present in \mathcal{K} .

as age thresholds, mental state, and subject qualification, into unified representations. Specifically, for triples describing the same legal concept but differing slightly in phrasing or numeric range, we perform abstraction and consolidation. For example, multiple expressions of different age intervals (e.g., “under 14,” “between 14 and 16”) are unified into a single category reflecting the statutory age of criminal responsibility. Likewise, triples involving exculpatory conditions such as self-defense and emergency avoidance are merged to represent a generalized justification element. Disjunctive (“or”) logic is preserved through semantic compression when legal equivalence holds, whereas conjunctive (“and”) logic necessitates the retention of separate triples. After semantic unification, a final filtering step removes knowledge unrelated to the formal reasoning structure of court judgments.

C. Knowledge Conversion and Graph Induction

The filtered set of triples \mathcal{A} is used to populate the leaf nodes of the procedural reasoning graph $\mathcal{G} = g_i$, which defines the structural flow of inference but lacks concrete factual content. Each triple $(h, r, t) \in \mathcal{A}$ is first mapped by a mapper module \mathcal{M} to a unique leaf node $d \in \mathcal{D}_i^*$ in the corresponding Reasoning Graph $\mathcal{K}'_i = (\mathcal{D}_i, \mathcal{P}_i, \mathcal{S}_i, \mathcal{F}_i)$. This produces a set of alignment pairs $\mathcal{A} = ((h, r, t), d)$ that indicate which factual triple supports which decision node.

These alignment pairs \mathcal{A} are then passed as priors to a lexicalizer module \mathcal{L} , which converts each triple into a natural language phrase p optimized for use in language models. The lexicalization process follows a strict formatting protocol: each phrase must be semantically precise, syntactically minimal, and free of extraneous punctuation, line breaks, or metadata. Numerical expressions are preserved in their original form to maintain factual accuracy.

The resulting phrases are inserted into the Reasoning Graph by establishing supporting edges $(p, d) \in \mathcal{S}_i$ from the lexicalized premise p to the corresponding reasoning node d . This completes the construction of the extended knowledge graph $\mathcal{K}' = \mathcal{K}'_i$, enriching the procedural skeleton \mathcal{G} with grounded factual support that is semantically aligned with domain-specific reasoning.

D. Alignment Evaluation

To assess whether the automatically generated graphs \mathcal{K}' can effectively replicate the semantic content of expert-annotated

⁶https://docs.llamaindex.ai/en/stable/api_reference/node_parsers/sentence_splitter/

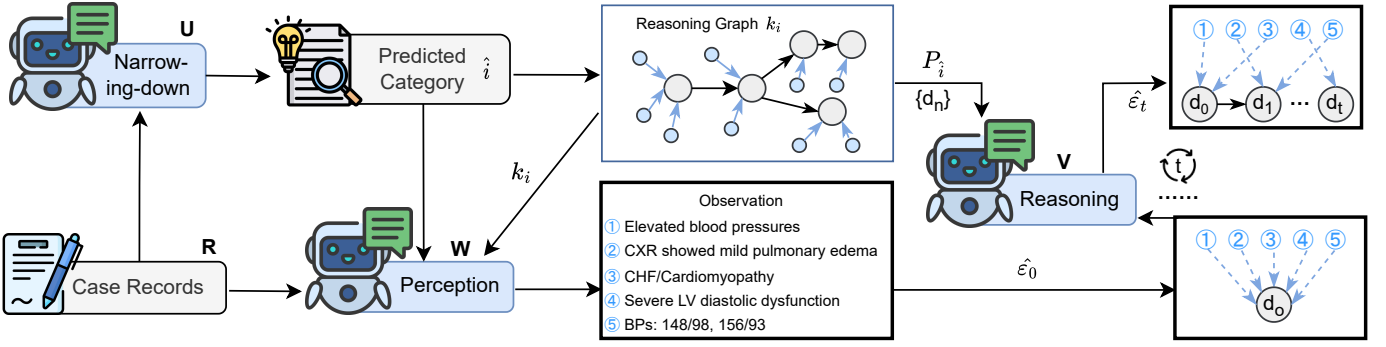


Fig. 6. Pipeline of our Graph-Based baseline. The dotted line in the right-most boxes means deductions from an observation to a decision.

graphs \mathcal{K} , we introduce a consistency evaluation metric based on semantic matching.

Let \mathcal{P} be the set of lexicalized knowledge phrases in the expert-defined graph \mathcal{K} , and let \mathcal{P}' be the set of knowledge phrases in the automatically generated graph \mathcal{K}' .

We begin by encoding each phrase $p \in \mathcal{P}$ and $p' \in \mathcal{P}'$ into a dense vector representation using a sentence encoder ϕ :

$$\mathbf{v}_p = \phi(p), \quad \mathbf{v}_{p'} = \phi(p')$$

Next, we compute the cosine similarity between all pairs $(p, p') \in \mathcal{P} \times \mathcal{P}'$:

$$s(p, p') = \frac{\phi(p) \cdot \phi(p')}{\|\phi(p)\| \cdot \|\phi(p')\|}$$

We define a match between p and p' if their similarity exceeds a threshold τ :

$$(p, p') \text{ is a match if } s(p, p') \geq \tau$$

A greedy maximum matching algorithm is then applied: among all unmatched pairs (p, p') that satisfy the threshold condition, we iteratively select the pair with the highest similarity, add it to the match set, and remove p and p' from further consideration. Let $\mathcal{C} \subseteq \mathcal{P} \times \mathcal{P}'$ denote the final set of matched pairs. We then compute the following metrics:

$$\text{Precision} = \frac{|\mathcal{C}|}{|\mathcal{P}'|}, \quad \text{Recall} = \frac{|\mathcal{C}|}{|\mathcal{P}|}$$

These metrics quantify the semantic alignment between the generated graph and the expert-defined gold standard: precision reflects the correctness of generated phrases, while recall measures the degree of recovery of expert knowledge.

V. BASELINE

We introduce two baselines that share a modular design but differ in whether they leverage a predefined reasoning graph. Both follow an iterative reasoning process with large language models (LLMs), but one explicitly traverses a graph while the other relies on free-form generation, optionally augmented by retrieval.

A. Graph-Based Baseline

Figure 6 provides an overview of our graph-based baseline, which comprises three LLM-based modules: narrowing-down (U), perception (W), and reasoning (V). In our experiments, each module utilizes the same type of LLM with different prompts (refer to the supplementary material for more details). U analyzes the entire case record R to determine the possible category \hat{i} (e.g., disease or offense type). W extracts observations that may lead to a final decision from each $r \in R$, producing a list of original decision-relevant descriptions. V iteratively derives possible decisions from observations based on the reasoning graph, providing rationales for each deduction (o, z, d) .

The narrowing-down module U takes R as input to make a prediction \hat{i} of the category, i.e., $\hat{i} = U(R)$. Let $d_t \in \mathcal{D}_{\hat{i}}$ be the decision that has been reached with t iterations over $k_{\hat{i}}$, where t corresponds to the depth of node d_t and so is less than or equal to the depth of $k_{\hat{i}}$. d_0 is the root node of $k_{\hat{i}}$. For d_0 , we apply the perception module to extract all observations in R and explanation \mathcal{E}_0 to support d_0 as

$$\hat{\mathcal{O}}, \hat{\mathcal{E}}_0 = W(d_0, k_{\hat{i}}). \quad (1)$$

$k_{\hat{i}}$ is supplied to facilitate the model to extract all observations for the following reasoning process.⁷

After the perception module W (iteration $t = 0$), we obtain all observations $\hat{\mathcal{O}}$, the root node of the decision process d_0 , and an explanation $\hat{\mathcal{E}}_0$ for the initial iteration. Assuming that by iteration t , we already know the decision for iteration t as d_t . $\{d_n\}$ is the set of d_t 's children, and $\mathcal{P}_{\hat{i}}(\{d_n\})$ represents the corresponding premises that support each d_n . V identifies the decision for the next step, d_{t+1} , and provides a justification \mathcal{E}_{t+1} . V will verify if there is any \hat{o} in $\hat{\mathcal{O}}$ that supports a d_n . If fully supported, d_n is identified as d_{t+1} for the $(t+1)$ -th iteration, i.e.,

$$d_{t+1}, \hat{\mathcal{E}}_{t+1} = V(\hat{\mathcal{O}}, \{d_n\}, \mathcal{P}_{\hat{i}}(\{d_n\})), \quad (2)$$

V continues until d_{t+1} in \mathcal{D}^* is identified. If no observation supports a d_n , the reasoning process will be stopped.

In our annotation, an observation o is associated with only one decision node d . However, our method employs an

⁷We used only pairs of an observation and a premise. We abuse \mathcal{K} to mean this for notational simplicity. The perception model can also utilize g_i instead of k_i for the first task.

TABLE III

EVALUATION BY MODEL ACROSS DIFFERENT REASONING SETTINGS (MEAN; SUBSCRIPTS DENOTE STD) ON MEDICAL DOMAIN. GREEN SHADING INDICATES VALUES THAT OUTPERFORM THE “WITH \mathcal{G} ” BASELINE; BOLDFACE INDICATES THE BEST VALUE WITHIN EACH COLUMN ACROSS ALL MODELS; UNDERLINE INDICATES THE BEST VALUE FOR EACH MODEL ACROSS ITS OWN SETTINGS.

Model	Baseline	Decision		Observation			Explanation	
		Acc^{cat}	Acc^{dec}	Obs^{pre}	Obs^{rec}	Obs^{comp}	Exp^{com}	Exp^{all}
LLaMA3.1 8B	with \mathcal{K}	0.327	0.237	0.096 ± 0.103	0.302 ± 0.267	0.089 ± 0.095	<u>0.177</u> ± 0.298	0.026 ± 0.051
	with \mathcal{K}'	0.333	0.203	0.097 ± 0.100	0.279 ± 0.241	0.087 ± 0.090	<u>0.171</u> ± 0.288	0.021 ± 0.037
	with \mathcal{K}^9	0.329	0.196	0.074 ± 0.085	0.259 ± 0.241	0.066 ± 0.075	<u>0.128</u> ± 0.246	0.014 ± 0.030
	with \mathcal{G}	0.339	0.184	<u>0.170</u> ± 0.148	0.378 ± 0.276	0.154 ± 0.134	<u>0.150</u> ± 0.254	0.036 ± 0.063
	ZS	0.329	0.024	0.161 ± 0.147	0.359 ± 0.280	0.146 ± 0.133	0.138 ± 0.265	0.035 ± 0.071
	RAG	0.325	0.006	0.126 ± 0.115	0.378 ± 0.287	0.118 ± 0.110	0.127 ± 0.251	0.023 ± 0.048
	G-RAG	0.329	0.045	0.111 ± 0.099	<u>0.432</u> ± 0.311	0.107 ± 0.094	0.115 ± 0.217	0.020 ± 0.040
LLaMA3.3 70B	with \mathcal{K}	0.571	0.570	0.271 ± 0.128	<u>0.598</u> ± 0.167	0.257 ± 0.126	<u>0.386</u> ± 0.368	<u>0.109</u> ± 0.117
	with \mathcal{K}'	0.562	0.522	0.273 ± 0.137	0.566 ± 0.182	0.255 ± 0.135	<u>0.371</u> ± 0.361	<u>0.103</u> ± 0.113
	with \mathcal{K}^9	0.568	0.528	0.255 ± 0.128	<u>0.588</u> ± 0.173	0.242 ± 0.128	<u>0.323</u> ± 0.331	0.082 ± 0.091
	with \mathcal{G}	0.570	0.503	0.284 ± 0.139	0.589 ± 0.187	0.268 ± 0.138	<u>0.274</u> ± 0.325	0.080 ± 0.102
	ZS	0.570	0.104	<u>0.285</u> ± 0.138	0.592 ± 0.187	<u>0.269</u> ± 0.137	0.200 ± 0.244	0.062 ± 0.084
	RAG	0.570	0.102	0.266 ± 0.128	0.613 ± 0.169	<u>0.253</u> ± 0.125	0.205 ± 0.241	0.059 ± 0.078
	G-RAG	0.566	0.151	0.223 ± 0.112	<u>0.618</u> ± 0.171	0.214 ± 0.108	0.197 ± 0.245	0.048 ± 0.067
GPT-4o	with \mathcal{K}	0.573	0.315	<u>0.463</u> ± 0.200	0.427 ± 0.209	0.349 ± 0.192	<u>0.446</u> ± 0.418	<u>0.179</u> ± 0.202
	with \mathcal{K}'	0.573	0.323	0.455 ± 0.204	0.370 ± 0.190	0.318 ± 0.183	<u>0.419</u> ± 0.408	0.151 ± 0.175
	with \mathcal{K}^9	0.570	0.274	0.454 ± 0.212	0.365 ± 0.199	0.318 ± 0.189	<u>0.413</u> ± 0.402	0.149 ± 0.172
	with \mathcal{G}	0.573	0.485	<u>0.469</u> ± 0.196	<u>0.528</u> ± 0.185	<u>0.398</u> ± 0.188	0.335 ± 0.357	0.148 ± 0.176
	ZS	0.573	0.029	0.450 ± 0.239	0.274 ± 0.192	0.257 ± 0.190	0.336 ± 0.419	0.090 ± 0.129
	RAG	0.573	0.010	0.423 ± 0.240	0.216 ± 0.169	0.208 ± 0.166	0.182 ± 0.337	0.043 ± 0.084
	G-RAG	0.573	0.096	0.335 ± 0.211	0.232 ± 0.168	0.186 ± 0.139	0.092 ± 0.239	0.020 ± 0.054
Claude 3.5 Haiku	with \mathcal{K}	0.554	0.472	0.251 ± 0.127	<u>0.557</u> ± 0.199	0.235 ± 0.121	<u>0.321</u> ± 0.331	0.086 ± 0.097
	with \mathcal{K}'	0.552	0.475	0.281 ± 0.140	<u>0.554</u> ± 0.196	0.261 ± 0.133	<u>0.328</u> ± 0.326	<u>0.098</u> ± 0.106
	with \mathcal{K}^9	0.552	0.483	0.249 ± 0.128	0.553 ± 0.200	0.233 ± 0.121	<u>0.317</u> ± 0.328	<u>0.086</u> ± 0.097
	with \mathcal{G}	0.562	0.475	0.287 ± 0.141	0.554 ± 0.184	0.264 ± 0.131	<u>0.279</u> ± 0.303	0.084 ± 0.100
	ZS	0.560	0.020	<u>0.301</u> ± 0.234	0.128 ± 0.121	0.119 ± 0.115	0.040 ± 0.172	0.007 ± 0.031
	RAG	0.556	0.012	0.251 ± 0.227	0.105 ± 0.105	0.097 ± 0.100	0.032 ± 0.150	0.005 ± 0.024
	G-RAG	0.562	0.061	0.173 ± 0.212	0.059 ± 0.082	0.058 ± 0.077	0.005 ± 0.061	0.001 ± 0.012
Claude 3.5 Sonnet	with \mathcal{K}	0.581	0.575	0.373 ± 0.167	<u>0.566</u> ± 0.182	0.341 ± 0.165	<u>0.393</u> ± 0.348	<u>0.148</u> ± 0.147
	with \mathcal{K}'	0.577	0.562	<u>0.396</u> ± 0.173	0.541 ± 0.185	<u>0.351</u> ± 0.166	<u>0.435</u> ± 0.376	<u>0.169</u> ± 0.165
	with \mathcal{K}^9	0.577	0.566	0.371 ± 0.166	0.563 ± 0.181	0.338 ± 0.162	<u>0.390</u> ± 0.347	<u>0.144</u> ± 0.143
	with \mathcal{G}	0.581	0.552	0.385 ± 0.164	0.568 ± 0.178	0.348 ± 0.159	0.320 ± 0.320	0.123 ± 0.134
	ZS	0.583	0.161	<u>0.386</u> ± 0.165	0.562 ± 0.177	0.344 ± 0.154	0.299 ± 0.303	0.115 ± 0.128
	RAG	0.581	0.145	<u>0.392</u> ± 0.167	0.563 ± 0.172	<u>0.350</u> ± 0.159	0.274 ± 0.291	0.105 ± 0.121
	G-RAG	0.585	0.147	0.351 ± 0.152	<u>0.613</u> ± 0.167	0.328 ± 0.148	0.252 ± 0.268	0.095 ± 0.113
Claude 3.7 Sonnet	with \mathcal{K}	0.552	0.570	0.367 ± 0.166	<u>0.598</u> ± 0.202	0.340 ± 0.159	<u>0.300</u> ± 0.310	<u>0.117</u> ± 0.132
	with \mathcal{K}'	0.552	0.546	0.385 ± 0.174	0.581 ± 0.197	0.352 ± 0.165	<u>0.333</u> ± 0.335	<u>0.134</u> ± 0.152
	with \mathcal{K}^9	0.552	0.570	0.365 ± 0.169	<u>0.593</u> ± 0.203	0.337 ± 0.158	<u>0.304</u> ± 0.315	<u>0.118</u> ± 0.132
	with \mathcal{G}	0.558	0.562	0.414 ± 0.190	0.579 ± 0.197	0.375 ± 0.183	0.272 ± 0.302	0.113 ± 0.140
	ZS	0.562	0.241	<u>0.416</u> ± 0.184	0.579 ± 0.192	<u>0.376</u> ± 0.179	0.225 ± 0.266	0.096 ± 0.126
	RAG	0.554	0.205	0.383 ± 0.173	0.568 ± 0.199	0.344 ± 0.158	0.193 ± 0.254	0.077 ± 0.109
	G-RAG	0.558	0.227	0.361 ± 0.164	<u>0.607</u> ± 0.189	0.335 ± 0.155	0.177 ± 0.232	0.072 ± 0.102

iterative reasoning pipeline. Initially, the perception module W generates an explanation set $\hat{\mathcal{E}}_0$, linking all \hat{o} to d_0 . During the t -th iteration of V , the explanation set is $\hat{\mathcal{E}}_t$, where at least one \hat{o} is linked to d_t . The final decision explanation is the combination of $\hat{\mathcal{E}}_0, \dots, \hat{\mathcal{E}}_T$ and d_0, \dots, d_T , where T represents the final iteration. In this combination, if an \hat{o} is eventually processed in the iteration for $\hat{\mathcal{E}}_t$, the corresponding (o, z, d) in all preceding $\hat{\mathcal{E}}_0, \dots, \hat{\mathcal{E}}_{t-1}$ will be removed. That is, \hat{o} will always be possessed by the d_t closest to the leaf node in the reasoning graph.

B. Free-form Baseline

In contrast to the graph-based approach, we propose a free-form baseline that shares a similar modular design but does not rely on a predefined reasoning graph. It begins with the same narrowing-down module U , which analyzes the case record R to predict a category \hat{i} , i.e., $\hat{i} = U(R)$. This prediction provides a high-level context, such as the disease or offense type, which can help condition downstream reasoning.

Optionally, a retrieval module \mathcal{R} is used to obtain guideline documents relevant to the case and predicted category: $\hat{G} = \mathcal{R}(R, \hat{i})$. These retrieved passages \hat{G} are appended to the model's input along with the original case record and a

TABLE IV

EVALUATION BY MODEL ACROSS DIFFERENT REASONING SETTINGS (MEAN; SUBSCRIPTS DENOTE STD) ON LEGEL DOMAIN. GREEN SHADING INDICATES VALUES THAT OUTPERFORM THE “WITH \mathcal{G} ” BASELINE; BOLDFACE INDICATES THE BEST VALUE WITHIN EACH COLUMN ACROSS ALL MODELS; UNDERLINE INDICATES THE BEST VALUE FOR EACH MODEL ACROSS ITS OWN SETTINGS.

Model	Baseline	Decision		Observation			Explanation	
		Acc^{cat}	Acc^{decs}	Obs^{pre}	Obs^{rec}	Obs^{comp}	Exp^{com}	Exp^{all}
LLaMA3.1 8B	with \mathcal{K}	<u>0.116</u>	<u>0.116</u>	0.064 \pm 0.134	0.064 \pm 0.138	<u>0.042</u> \pm 0.097	<u>0.022</u> \pm 0.119	<u>0.005</u> \pm 0.028
	with \mathcal{K}'	0.081	0.081	<u>0.073</u> \pm 0.156	<u>0.070</u> \pm 0.146	<u>0.048</u> \pm 0.111	0.006 \pm 0.054	0.001 \pm 0.011
	with \mathcal{G}	0.046	0.046	0.038 \pm 0.111	0.033 \pm 0.090	0.020 \pm 0.054	0.000 \pm 0.000	0.000 \pm 0.000
LLaMA3.3 70B	with \mathcal{K}	<u>0.500</u>	<u>0.442</u>	0.260 \pm 0.187	0.274 \pm 0.203	0.188 \pm 0.150	0.112 \pm 0.232	0.027 \pm 0.056
	with \mathcal{K}'	0.512	0.454	0.212 \pm 0.176	0.228 \pm 0.193	0.151 \pm 0.132	0.102 \pm 0.240	0.023 \pm 0.057
	with \mathcal{G}	0.488	0.430	0.236 \pm 0.190	0.252 \pm 0.208	0.171 \pm 0.154	0.077 \pm 0.206	0.015 \pm 0.037
GPT-4o	with \mathcal{K}	0.256	0.233	0.105 \pm 0.177	0.086 \pm 0.137	0.064 \pm 0.110	<u>0.072</u> \pm 0.186	<u>0.015</u> \pm 0.045
	with \mathcal{K}'	0.151	0.140	0.075 \pm 0.148	0.060 \pm 0.123	0.045 \pm 0.092	0.021 \pm 0.098	0.004 \pm 0.020
	with \mathcal{G}	<u>0.361</u>	<u>0.337</u>	<u>0.183</u> \pm 0.224	<u>0.136</u> \pm 0.168	<u>0.110</u> \pm 0.138	0.033 \pm 0.112	0.011 \pm 0.036
DeepSeek-v3	with \mathcal{K}	<u>0.337</u>	<u>0.279</u>	<u>0.161</u> \pm 0.212	<u>0.228</u> \pm 0.207	<u>0.095</u> \pm 0.141	<u>0.065</u> \pm 0.159	<u>0.017</u> \pm 0.042
	with \mathcal{K}'	0.302	0.244	0.125 \pm 0.183	0.141 \pm 0.207	<u>0.095</u> \pm 0.141	<u>0.065</u> \pm 0.159	<u>0.017</u> \pm 0.042
	with \mathcal{G}	0.140	0.105	0.046 \pm 0.119	0.043 \pm 0.107	0.032 \pm 0.080	0.027 \pm 0.134	0.007 \pm 0.035

few-shot example set \mathcal{X} .

The free-form reasoning process proceeds iteratively. At each step t , the model uses the full context, including R , \hat{G} , previous predictions d'_0, \dots, d'_{t-1} , and \mathcal{X} to generate the next decision d'_t and its explanation $\hat{\mathcal{E}}_t$:

$$d'_t, \hat{\mathcal{E}}_t = \mathcal{F}(R, \hat{G}, d'_0, \dots, d'_{t-1}, \mathcal{X}). \quad (3)$$

Unlike the graph-based setting, there is no explicit traversal of a decision tree; the model freely decides what to predict and when to stop, up to a fixed iteration limit T for consistency in evaluation.

To enable comparison with the graph-based model, we apply a post-hoc alignment module \mathcal{H} that maps each free-form decision d'_t to a node $d_t \in \mathcal{D}$ in the gold reasoning graph:

$$d_t = \mathcal{H}(d'_t, \mathcal{D}). \quad (4)$$

The alignment is based on semantic content and graph position. The final output is a decision chain d_0, \dots, d_T and explanation set $\hat{\mathcal{E}} = \bigcup_{t=0}^T \hat{\mathcal{E}}_t$. This design enables unconstrained reasoning while remaining evaluable under structured metrics.

VI. EXPERIMENTS

A. Experimental Setup

We evaluate the reasoning capabilities of seven recent LLMs from both open-source and commercial families. In the medical domain, our evaluation includes six instruction-tuned models: the open-source LLMs **Llama-3.1-8B-Instruct**⁸ and **Llama-3.3-70B-Instruct**⁹, as well as the commercial LLMs **GPT-4o**¹⁰, **Claude 3.5 Haiku**¹¹, **Claude 3.5 Sonnet**¹², and

⁸<https://huggingface.co/meta-llama/Llama-3.1-8B>

⁹<https://huggingface.co/meta-llama/Llama-3.3-70B-Instruct>

¹⁰Version: gpt-4o-2024-11-20, <https://learn.microsoft.com/en-us/azure/ai-services/openai/concepts/models>

¹¹Version: claude-3-5-haiku-20241022, <https://docs.anthropic.com/en/docs/agents-and-tools/tool-use/computer-use-tool>

¹²Version: claude-3-5-sonnet-20241022, same source as above

Claude 3.7 Sonnet¹³ (reasoning models with internal thinking processes)¹⁴. In the legal domain, since the primary goal is to evaluate the generalizability of our baseline and semi-automatic annotation workflow, we select a representative subset of the above models (**Llama-3.1-8B-Instruct**, **Llama-3.3-70B-Instruct**, and **GPT-4o**); additionally, because all legal documents are in Chinese, we include **DeepSeek-V3**¹⁵ for its strong Chinese language capabilities.

All these models are used to instantiate the narrowing-down, perception, and reasoning modules in our baseline pipeline. The temperature is fixed at 0 to ensure deterministic outputs. We conduct experiments across seven reasoning settings: with reasoning graphs (\mathcal{K}), with automatically constructed reasoning graphs (\mathcal{K}'_o , \mathcal{K}'), with procedural graphs(\mathcal{G}), and unstructured variants including zero-shot prompting (ZS), with retrieval-augmented generation (RAG), and with graph RAG (G-RAG)¹⁶. For RAG, we use BM25 with default parameters to retrieve the top 5 passages (each truncated to 512 tokens). For G-RAG, retrieval follows the public implementation, with LLaMA3.1 8B used for graph construction and query generation, retrieving the top 5 passages (each truncated to 512 tokens). All these settings are evaluated in the medical domain. In the legal domain, since the primary goal is to evaluate the generalizability of our baseline and the semi-automatic annotation workflow, we only conduct experiments on the first three settings: with reasoning graphs (\mathcal{K}), with automatically constructed reasoning graphs (\mathcal{K}'), and with procedural subgraphs (\mathcal{G}).

¹³Version: claude-3-7-sonnet-20250219, same source as above

¹⁴All above models are evaluated in HIPAA-compliant environments that ensure no data is transferred to third-party providers such as Microsoft or OpenAI. This secure setup enables us to conduct experiments involving the MIMIC-IV dataset in full compliance with its Data Use Agreement.

¹⁵Version: deepseek-v3-250325, <https://api-docs.deepseek.com/zh-cn/news/news250325>

¹⁶G-RAG is adapted from <https://github.com/gusye1234/nano-graphrag>.

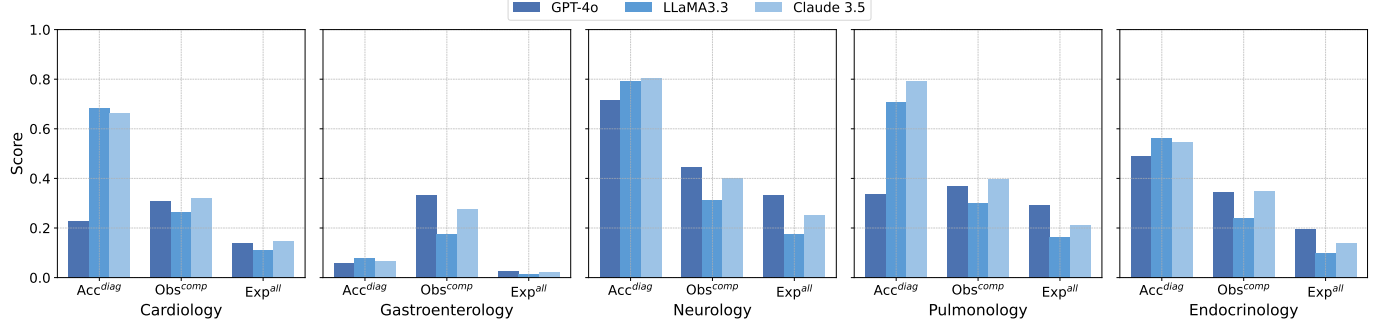


Fig. 7. Performance of GPT-4o, Claude 3.5, and LLaMA3 70B across different medical domains. Evaluated with Acc^{decs} (Accuracy), Obs^{comp} (Comp), and Exp^{all} (Faith).

For our semi-automatic annotation workflow, we consistently employ Llama-3.3-70B-Instruct across all components: the extractor (\mathcal{E}), filter (\mathcal{F}), mapper (\mathcal{M}), and lexicalizer (\mathcal{L}). It is also used to implement the post-hoc alignment module \mathcal{H} in the free-form baseline. To assess the upper bound of our approach, we further generate an enhanced variant \mathcal{K}'_o in the medical domain using a stronger model, GPT-4o. The sentence encoder ϕ is chosen per domain to balance accuracy and efficiency. In the legal domain, we use `ritrieve_zh_v1`¹⁷ for encoding legal phrases. In the medical domain, we adopt bilingual-document-embedding-large¹⁸. For reasoning-based evaluations, we use Llama-3-8B-Instruct with few-shot prompts to align and verify observation and explanation predictions. Additional implementation details and prompts are provided in the supplementary material.

B. Experimental Results

Table III presents the main experimental results in the medical domain across all reasoning settings. Among all settings, the best performance is consistently achieved when models are equipped with expert-annotated reasoning graphs (\mathcal{K}). This setting yields the highest scores across all core metrics, including diagnostic accuracy, observation completeness, and explanation faithfulness. For instance, with fully annotated graphs, LLaMA3.3 70B reaches an Acc^{decs} of 0.570 and an Exp^{all} of 0.109, while Claude 3.5 Sonnet achieves an Acc^{decs} of 0.575 and an Exp^{all} of 0.148. In terms of specific capabilities, GPT-4o obtains the highest scores in observation extraction (Obs^{pre} of 0.463) and explanation quality (Exp^{all} of 0.179). In contrast, Claude 3.5 Sonnet excels in diagnostic accuracy in some settings.

Comparing settings, models augmented with knowledge related to reasoning significantly outperform those using only procedural graphs (\mathcal{G}) in accurately predicting final decisions and generating explanations consistent with those of human experts. The inclusion of knowledge related to reasoning not only enhances diagnostic accuracy but also leads to more complete and faithful explanations. Automatically constructed reasoning graphs (\mathcal{K}') show clear gains over procedural graphs;

for example, LLaMA3.3 70B achieves an Acc^{decs} of 0.528 with \mathcal{K}' compared to 0.503 with \mathcal{G} , demonstrating the practical value of semi-automatic annotation. In the legal dataset, the same pattern holds: models using automatically constructed graphs achieve higher scores than those relying solely on procedural logic, confirming the generalizability of the semi-automatic annotation pipeline and reasoning graph framework. Although automatically constructed graphs still lag behind expert annotation, leveraging stronger LLMs such as GPT-4o for graph construction (\mathcal{K}'_o) can further narrow the gap, as reflected by improved explanation metrics (e.g., GPT-4o achieves Exp^{all} of 0.151 in the \mathcal{K}'_o setting). This suggests that improving the underlying LLM can further enhance the quality of automatic annotations. When comparing structured graph-based approaches with unstructured methods such as Zero-Shot (ZS), Retrieval-Augmented Generation (RAG), and Graph-RAG (G-RAG), the gap is even more pronounced. Unstructured methods consistently underperform across all metrics; for example, GPT-4o's Acc^{decs} is only 0.029 in the ZS setting, showing that explicit graph-based knowledge is essential for complex reasoning.

Looking at model comparisons, larger models such as LLaMA3.3 70B and Claude 3.5 Sonnet consistently outperform smaller models like LLaMA3.1 8B and Claude 3.5 Haiku across nearly all evaluated metrics. While GPT-4o demonstrates strong performance in observation extraction and explanation quality, Claude 3.5 Sonnet sometimes surpasses it in diagnostic accuracy, indicating that higher capacity and different model architectures may yield advantages in specific reasoning tasks. It is also noteworthy that Claude 3.7 Sonnet, despite its reasoning-oriented design, performs slightly worse than Claude 3.5 Sonnet in most metrics, suggesting that introducing explicit thinking steps alone does not guarantee comprehensive improvements in multi-step reasoning performance. Overall, model scale and structure both play important roles, and no single model dominates in all dimensions.

In summary, these results demonstrate that integrating structured external knowledge, whether through expert annotation or high-quality automatic construction, significantly boosts LLM reasoning capabilities in both medical and legal domains. Nonetheless, current models still show limitations in aligning with expert reasoning and producing fully faithful explanations, suggesting that further advancements in model architecture and scalable knowledge distillation are required

¹⁷https://huggingface.co/richinfoai/ritrieve_zh_v1, a Chinese retrieval model optimized for legal semantics.

¹⁸<https://huggingface.co/Lajavaness/bilingual-document-embedding>, a bilingual model effective for semantic alignment in clinical texts.

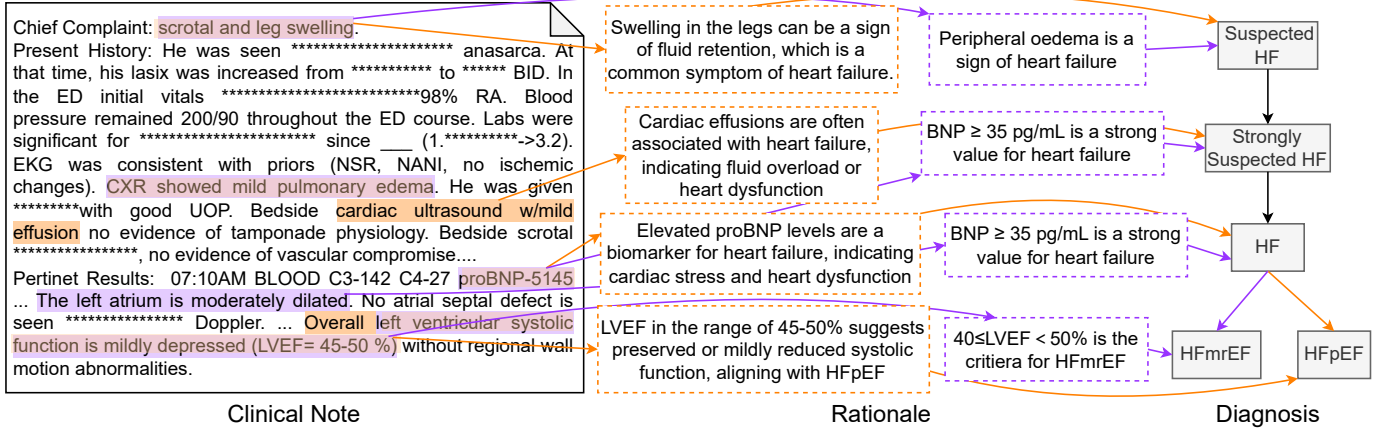


Fig. 8. An example prediction for a case record with final decision of Heart Failure (HF) by GPT-4o.

TABLE V

SEMANTIC ALIGNMENT (RECALL AND PRECISION) OF SEMI-AUTOMATICALLY CONSTRUCTED REASONING GRAPHS WITH EXPERT-ANNOTATED GRAPHS ACROSS DOMAINS AND ANNOTATOR MODELS.

Setting	Recall	Precision
Medical (LLaMA3.7 70B)	0.8203	0.2351
Medical (GPT-4o)	0.7250	0.3405
Legal (LLaMA3.3 70B)	0.9583	0.6181

to achieve expert-level performance.

C. Performance across Medical Domains

Figure 7 presents the performance of models across different medical domains, demonstrating clear differences in the ability of LLMs to utilize knowledge resources depending on the field. Specifically, models achieve relatively higher diagnostic accuracy in domains such as Neurology and Cardiology, while performance is noticeably lower in areas like Gastroenterology. Despite these differences in diagnostic outcomes, faithfulness in explanation remains consistently low across all domains and models. This indicates that even when models perform well in terms of accuracy for certain specialties, they still struggle to produce clinically meaningful and faithful explanations, highlighting a persistent challenge in model interpretability.

D. Alignment Evaluation between \mathcal{K}' and \mathcal{K}

To compare the alignment between semi-automatically constructed reasoning graphs (\mathcal{K}') and the corresponding expert-constructed graphs (\mathcal{K}), we evaluate both recall and precision. As shown in Table V, in the medical domain, LLaMA3.3 70B achieves a recall of 0.8203 and a precision of 0.2351, while GPT-4o attains a slightly lower recall of 0.725 but a substantially higher precision of 0.3405. This indicates that although both models achieve a high overall match with expert knowledge, GPT-4o produces more precise graphs with fewer irrelevant or redundant connections. In the legal domain, LLaMA3.3 70B achieves both higher recall (0.9583) and higher precision (0.6181), suggesting that the semi-automatic

TABLE VI

CONSISTENCY OF AUTOMATED EVALUATION WITH HUMAN JUDGMENTS. EVALUATED BY MEAN AND CONFIDENCE INTERVAL (CI).

Model	Observation		Rationalization	
	Mean	95% CI	Mean	95% CI
LLama3 8B	0.887	0.844 ~ 0.878	0.835	0.759 ~ 0.818
GPT-4 turbo	0.902	0.830 ~ 0.863	0.876	0.798 ~ 0.853

annotation pipeline aligns particularly well in the law domain. Overall, these results demonstrate that while semi-automatic annotation can introduce some redundant information, it is capable of recovering most expert knowledge. Moreover, leveraging more powerful models such as GPT-4o can further improve the specificity and precision of automatically constructed graphs, thereby narrowing the gap with expert annotation.

E. Reliability of Automatic Evaluation

We randomly pick out 100 samples from the medical domain and their prediction by GPT-4o over the task with \mathcal{G} to assess the consistency of our automated metrics to evaluate the observational and explanatory performance in Section III-C with human judgments.

Three physicians joined this experiment. For each prediction $\hat{o} \in \hat{\mathcal{O}}$, they are asked to find a similar observation in the ground truth \mathcal{O} . For explanatory metrics, they verify if each prediction $\hat{z} \in \hat{\mathcal{E}}$ for $\hat{o} \in \hat{\mathcal{O}}$ align with ground-truth $z \in \mathcal{E}$ corresponding to o . A prediction and a ground truth are deemed aligned for both assessments if at least two specialists agree. We compare LLama3's and GPT-4's judgments to explore if there is a gap between these LLMs. As summarized in Table VI, GPT-4 achieves the best results, with LLama3 8B also displaying a similar performance. From these results, we argue that our automated evaluation metrics are consistent with human judgments, and LLama3 is sufficient for this evaluation, allowing the cost-efficient option. Detailed analysis is available in the supplementary material.

F. Prediction examples.

Figure 8 presents an example prediction by GPT-4o, where the model concludes a diagnosis of Heart Failure (HF), whereas the actual label is Suspected HF. In this figure, red highlights shared rationale between prediction and ground truth, while purple and orange denote rationale found only in the ground truth or prediction, respectively. GPT-4o places strong emphasis on features such as elevated proBNP levels and lower LVEF (45{50%), which support a classification of HFmrEF or HFpEF. However, some of these markers, like mild systolic dysfunction and moderate left atrial dilation, may still be ambiguous and better interpreted as indicators of possible or suspected HF rather than a confirmed case. The model’s over-reliance on partially indicative features, while discounting clinical hedges such as “no tamponade physiology” or stable EKG findings, results in over-diagnosis. Such misalignments between clinical nuance and model interpretation underscore GPT-4o’s challenges in reasoning under diagnostic uncertainty.

VII. CONCLUSION

In this work, we introduce REACT, a benchmark designed to evaluate whether LLMs can reach accurate conclusions and expert domain-aligned reasoning when grounded in real-world, a comprehensive framework for evaluating large language models (LLMs) on complex reasoning tasks in medicine and law. REACT addresses key limitations of existing benchmarks by focusing on three essential dimensions: evidence extraction from detailed case records, multi-step expert-aligned logical reasoning, and the generation of transparent, verifiable explanations. Our experiments show that structured knowledge representations, especially the proposed Reasoning Graphs, significantly improve performance. However, current state-of-the-art models still fall short of expert-level reasoning fidelity, and explanation faithfulness remains a major hurdle across all domains.

Looking ahead, several research avenues are critical. Advancing automatic graph induction techniques could close the gap between machine-generated and expert annotations. Additionally, developing model architectures that better integrate structured knowledge with free-form reasoning holds promise for improving both interpretability and accuracy. Extending the benchmark to support dynamic knowledge updates and adversarial testing will further enhance its real-world relevance. By releasing our dataset and tools, we aim to catalyze progress toward transparent, trustworthy AI in high-stakes fields, positioning REACT as a foundational resource for future research in interpretable and accountable AI.

REFERENCES

- [1] T. B. Brown, B. Mann, N. Ryder, M. Subbiah, J. Kaplan, P. Dhariwal, A. Neelakantan, P. Shyam, G. Sastry, A. Askell, S. Agarwal, A. Herbert-Voss, G. Krueger, T. Henighan, R. Child, A. Ramesh, D. M. Ziegler, J. Wu, C. Winter, C. Hesse, M. Chen, E. Sigler, M. Litwin, S. Gray, B. Chess, J. Clark, C. Berner, S. McCandlish, A. Radford, I. Sutskever, and D. Amodei, “Language models are few-shot learners,” in *Advances in Neural Information Processing Systems 33: Annual Conference on Neural Information Processing Systems 2020, NeurIPS 2020, December 6-12, 2020, virtual*, H. Larochelle, M. Ranzato, R. Hadsell, M. Balcan, and H. Lin, Eds., 2020. [Online]. Available: <https://proceedings.neurips.cc/paper/2020/hash/1457c0d6bfc4967418bf8ac142f64a-Abstract.html>
- [2] J. Wei, M. Bosma, V. Y. Zhao, K. Guu, A. W. Yu, B. Lester, N. Du, A. M. Dai, and Q. V. Le, “Finetuned language models are zero-shot learners,” in *The Tenth International Conference on Learning Representations, ICLR 2022, Virtual Event, April 25-29, 2022*, OpenReview.net, 2022. [Online]. Available: <https://openreview.net/forum?id=gEZrGCozdqR>
- [3] L. Ouyang, J. Wu, X. Jiang, D. Almeida, C. L. Wainwright, P. Mishkin, C. Zhang, S. Agarwal, K. Slama, A. Ray, J. Schulman, J. Hilton, F. Kelton, L. Miller, M. Simens, A. Askell, P. Welinder, P. F. Christiano, J. Leike, and R. Lowe, “Training language models to follow instructions with human feedback,” in *Advances in Neural Information Processing Systems 35: Annual Conference on Neural Information Processing Systems 2022, NeurIPS 2022, New Orleans, LA, USA, November 28 - December 9, 2022*, S. Koyejo, S. Mohamed, A. Agarwal, D. Belgrave, K. Cho, and A. Oh, Eds., 2022. [Online]. Available: http://papers.nips.cc/paper_files/paper/2022/hash/b1efde53be364a73914f58805a001731-Abstract-Conference.html
- [4] J. Liu, L. Li, T. Xiang, B. Wang, and Y. Qian, “Tcra-llm: Token compression retrieval augmented large language model for inference cost reduction,” in *Findings of the Association for Computational Linguistics: EMNLP 2023*, 2023, pp. 9796–9810.
- [5] J. Chen, B. Wang, Z. Jiang, and Y. Nakashima, “Putting people in llms’ shoes: Generating better answers via question rewriter,” in *AAAI-25, Sponsored by the Association for the Advancement of Artificial Intelligence, February 25 - March 4, 2025, Philadelphia, PA, USA*, T. Walsh, J. Shah, and Z. Kolter, Eds. AAAI Press, 2025, pp. 23 577–23 585. [Online]. Available: <https://doi.org/10.1609/aaai.v39i22.34527>
- [6] K. Singhal, S. Azizi, T. Tu, S. S. Mahdavi, J. Wei, H. W. Chung, N. Scales, A. K. Tanwanii, H. Cole-Lewis, S. Pfohl, P. Payne, M. Seneviratne, P. Gamble, C. Kelly, N. Schärlí, A. Chowdhery, P. A. Mansfield, B. A. y Arcas, D. R. Webster, G. S. Corrado, Y. Matias, K. Chou, J. Gottweis, N. Tomasev, Y. Liu, A. Rajkomar, J. K. Barral, C. Semturs, A. Karthikesalingam, and V. Natarajan, “Large language models encode clinical knowledge,” *CoRR*, vol. abs/2212.13138, 2022. [Online]. Available: <https://doi.org/10.48550/arXiv.2212.13138>
- [7] Z. Yi, J. Ouyang, Y. Liu, T. Liao, Z. Xu, and Y. Shen, “A survey on recent advances in llm-based multi-turn dialogue systems,” *CoRR*, vol. abs/2402.18013, 2024. [Online]. Available: <https://doi.org/10.48550/arXiv.2402.18013>
- [8] H. Duan, J. Wei, C. Wang, H. Liu, Y. Fang, S. Zhang, D. Lin, and K. Chen, “Botchat: Evaluating llms’ capabilities of having multi-turn dialogues,” in *Findings of the Association for Computational Linguistics: NAACL 2024, Mexico City, Mexico, June 16-21, 2024*, K. Duh, H. Gómez-Adorno, and S. Bethard, Eds. Association for Computational Linguistics, 2024, pp. 3184–3200. [Online]. Available: <https://doi.org/10.18653/v1/2024.findings-naacl.201>
- [9] B. Rozière, J. Gehring, F. Gloeckle, S. Sootla, I. Gat, X. E. Tan, Y. Adi, J. Liu, T. Remez, J. Rapin, A. Kozhevnikov, I. Evtimov, J. Bitton, M. Bhatt, C. Canton-Ferrer, A. Grattafiori, W. Xiong, A. Défosséz, J. Copet, F. Azhar, H. Touvron, L. Martin, N. Usunier, T. Scialom, and G. Synnaeve, “Code llama: Open foundation models for code,” *CoRR*, vol. abs/2308.12950, 2023. [Online]. Available: <https://doi.org/10.48550/arXiv.2308.12950>
- [10] B. Liu, C. Chen, Z. Gong, C. Liao, H. Wang, Z. Lei, M. Liang, D. Chen, M. Shen, H. Zhou, W. Jiang, H. Yu, and J. Li, “Mftcoder: Boosting code llms with multitask fine-tuning,” in *Proceedings of the 30th ACM SIGKDD Conference on Knowledge Discovery and Data Mining, KDD 2024, Barcelona, Spain, August 25-29, 2024*, R. Baeza-Yates and F. Bonchi, Eds. ACM, 2024, pp. 5430–5441. [Online]. Available: <https://doi.org/10.1145/3637528.3671609>
- [11] Z. Sadeghi, R. Alizadehsani, M. A. Cifci, S. Kausar, R. Rehman, P. Mahanta, P. K. Bora, A. Almasri, R. S. Alkhawaldeh, S. Hussain, B. Alatas, A. Shoeibi, H. Moosaei, M. Hladík, S. Nahavandi, and P. M. Pardalos, “A review of explainable artificial intelligence in healthcare,” *Comput. Electr. Eng.*, vol. 118, p. 109370, 2024. [Online]. Available: <https://doi.org/10.1016/j.compeleceng.2024.109370>
- [12] F. Doshi-Velez, M. Kortz, R. Budish, C. Bavitz, S. Gershman, D. O’Brien, S. Schieber, J. Waldo, D. Weinberger, and A. Wood, “Accountability of AI under the law: The role of explanation,” *CoRR*, vol. abs/1711.01134, 2017. [Online]. Available: <http://arxiv.org/abs/1711.01134>
- [13] A. Pal, L. K. Umapathi, and M. Sankarasubbu, “MedMCQA: A large-scale multi-subject multi-choice dataset for medical domain question answering,” in *Conference on health, inference, and learning*. PMLR, 2022, pp. 248–260.

[14] M. Jullien, M. Valentino, H. Frost, P. O'Regan, D. Landers, and A. Freitas, "Semeval-2023 task 7: Multi-evidence natural language inference for clinical trial data," *arXiv preprint arXiv:2305.02993*, 2023.

[15] H. Zhong, C. Xiao, C. Tu, T. Zhang, Z. Liu, and M. Sun, "JEC-QA: A legal-domain question answering dataset," in *The Thirty-Fourth AAAI Conference on Artificial Intelligence, AAAI 2020, The Thirty-Second Innovative Applications of Artificial Intelligence Conference, IAAI 2020, The Tenth AAAI Symposium on Educational Advances in Artificial Intelligence, EAAI 2020, New York, NY, USA, February 7-12, 2020*. AAAI Press, 2020, pp. 9701–9708. [Online]. Available: <https://doi.org/10.1109/aaai.v34i05.6519>

[16] C. Xiao, H. Zhong, Z. Guo, C. Tu, Z. Liu, M. Sun, Y. Feng, X. Han, Z. Hu, H. Wang, and J. Xu, "CAIL2018: A large-scale legal dataset for judgment prediction," *CoRR*, vol. abs/1807.02478, 2018. [Online]. Available: <http://arxiv.org/abs/1807.02478>

[17] B. Dalvi, P. Jansen, O. Tafjord, Z. Xie, H. Smith, L. Pipatanangkura, and P. Clark, "Explaining answers with entailment trees," in *Proceedings of the 2021 Conference on Empirical Methods in Natural Language Processing, EMNLP 2021, Virtual Event / Punta Cana, Dominican Republic, 7-11 November, 2021*, M. Moens, X. Huang, L. Specia, and S. W. Yih, Eds. Association for Computational Linguistics, 2021, pp. 7358–7370. [Online]. Available: <https://doi.org/10.18653/v1/2021.emnlp-main.585>

[18] G. Chen, K. Tang, C. Yang, F. Ye, Y. Qiao, and Y. Qian, "SEER: facilitating structured reasoning and explanation via reinforcement learning," in *Proceedings of the 62nd Annual Meeting of the Association for Computational Linguistics (Volume 1: Long Papers), ACL 2024, Bangkok, Thailand, August 11-16, 2024*, L. Ku, A. Martins, and V. Srikanth, Eds. Association for Computational Linguistics, 2024, pp. 5901–5921. [Online]. Available: <https://doi.org/10.18653/v1/2024.acl-long.321>

[19] A. E. W. Johnson, L. Bulgarelli, L. Shen, A. Gayles, A. Shammout, S. Hornig, T. J. Pollard, S. Hao, B. Moody, B. Gow, L.-w. H. Lehman, L. A. Celi, and R. G. Mark, "MIMIC-IV, a freely accessible electronic health record dataset," *Scientific data*, vol. 10, no. 1, p. 1, 2023.

[20] X. Chen and S. Wiseman, "BM25 query augmentation learned end-to-end," *CoRR*, vol. abs/2305.14087, 2023. [Online]. Available: <https://doi.org/10.48550/arXiv.2305.14087>

[21] D. Edge, H. Trinh, N. Cheng, J. Bradley, A. Chao, A. Mody, S. Truitt, and J. Larson, "From local to global: A graph RAG approach to query-focused summarization," *CoRR*, vol. abs/2404.16130, 2024. [Online]. Available: <https://doi.org/10.48550/arXiv.2404.16130>

[22] B. Wang, J. Chang, Y. Qian, G. Chen, J. Chen, Z. Jiang, J. Zhang, Y. Nakashima, and H. Nagahara, "Direct: Diagnostic reasoning for clinical notes via large language models," in *Advances in Neural Information Processing Systems 38: Annual Conference on Neural Information Processing Systems 2024, NeurIPS 2024, Vancouver, BC, Canada, December 10 - 15, 2024*, A. Globersons, L. Mackey, D. Belgrave, A. Fan, U. Paquet, J. M. Tomczak, and C. Zhang, Eds., 2024. [Online]. Available: http://papers.nips.cc/paper_files/paper/2024/hash/892850bf793e03b5c410dfd9425b94c8-Abstract-Datasets_and_Benchmarks_Track.html

[23] D. Li, J. Yu, B. Hu, Z. Xu, and M. Zhang, "ExplainCPE: A free-text explanation benchmark of chinese pharmacist examination," *arXiv preprint arXiv:2305.12945*, 2023.

[24] H. Chen, Z. Fang, Y. Singla, and M. Dredze, "Benchmarking large language models on answering and explaining challenging medical questions," *arXiv preprint arXiv:2402.18060*, 2024.

[25] Y. Gao, D. Dligach, T. Miller, S. Tesch, R. Laffin, M. M. Churpek, and M. Afshar, "Hierarchical annotation for building a suite of clinical natural language processing tasks: Progress note understanding," in *Proceedings of the Thirteenth Language Resources and Evaluation Conference*. Marseille, France: European Language Resources Association, 2022, pp. 5484–5493.

[26] T. Zack, G. Dhaliwal, R. Geha, M. Margaretten, S. Murray, and J. C. Hong, "A clinical reasoning-encoded case library developed through natural language processing," *Journal of General Internal Medicine*, vol. 38, no. 1, pp. 5–11, 2023.

[27] Y. Wang, X. Shen, Z. Huang, L. Niu, and S. Ou, "clegal-qa: a chinese legal question answering with natural language generation methods," *Complex & Intelligent Systems*, vol. 11, no. 1, p. 77, 2025.

[28] R. Bhambhoria, S. Dahan, J. Li, and X. Zhu, "Evaluating AI for law: Bridging the gap with open-source solutions," *CoRR*, vol. abs/2404.12349, 2024. [Online]. Available: <https://doi.org/10.48550/arXiv.2404.12349>

[29] A. Chen, F. Yao, X. Zhao, Y. Zhang, C. Sun, Y. Liu, and W. Shen, "EQUALS: A real-world dataset for legal question answering via reading chinese laws," in *Proceedings of the Nineteenth International Conference on Artificial Intelligence and Law, ICAIL 2023, Braga, Portugal, June 19-23, 2023*, M. Grabmair, F. Andrade, and P. Novais, Eds. ACM, 2023, pp. 71–80. [Online]. Available: <https://doi.org/10.1145/3594536.3595159>

[30] H. Ye, X. Jiang, Z. Luo, and W. Chao, "Interpretable charge predictions for criminal cases: Learning to generate court views from fact descriptions," *CoRR*, vol. abs/1802.08504, 2018. [Online]. Available: <http://arxiv.org/abs/1802.08504>

[31] L. Cao, Z. Wang, C. Xiao, and J. Sun, "PILOT: legal case outcome prediction with case law," in *Proceedings of the 2024 Conference of the North American Chapter of the Association for Computational Linguistics: Human Language Technologies (Volume 1: Long Papers), NAACL 2024, Mexico City, Mexico, June 16-21, 2024*, K. Duh, H. Gómez-Adorno, and S. Bethard, Eds. Association for Computational Linguistics, 2024, pp. 609–621. [Online]. Available: <https://doi.org/10.18653/v1/2024.nacl-long.34>

[32] J. Shen, J. Xu, H. Hu, L. Lin, F. Zheng, G. Ma, F. Meng, J. Zhou, and W. Han, "A law reasoning benchmark for LLM with tree-organized structures including factum probandum, evidence and experiences," *CoRR*, vol. abs/2503.00841, 2025. [Online]. Available: <https://doi.org/10.48550/arXiv.2503.00841>

[33] B. Min, H. Ross, E. Sulem, A. P. B. Veyseh, T. H. Nguyen, O. Sainz, E. Agirre, I. Heintz, and D. Roth, "Recent advances in natural language processing via large pre-trained language models: A survey," *ACM Computing Surveys*, vol. 56, no. 2, pp. 1–40, 2023.

[34] M. Danilevsky, K. Qian, R. Aharonov, Y. Katsis, B. Kawas, and P. Sen, "A survey of the state of explainable AI for natural language processing," in *Proceedings of the 1st Conference of the Asia-Pacific Chapter of the Association for Computational Linguistics and the 10th International Joint Conference on Natural Language Processing*, 2020, pp. 447–459.

[35] S. Gurrapu, A. Kulkarni, L. Huang, I. Lourentzou, and F. A. Batarseh, "Rationalization for explainable nlp: A survey," *Frontiers in Artificial Intelligence*, vol. 6, 2023.

[36] O.-M. Camburu, T. Rocktäschel, T. Lukasiewicz, and P. Blunsom, "e-snli: Natural language inference with natural language explanations," *Advances in Neural Information Processing Systems*, vol. 31, 2018.

[37] N. F. Rajani, B. McCann, C. Xiong, and R. Socher, "Explain yourself! leveraging language models for commonsense reasoning," in *Proceedings of the 57th Annual Meeting of the Association for Computational Linguistics*, Florence, Italy, 2019, pp. 4932–4942.

[38] J. DeYoung, S. Jain, N. F. Rajani, E. Lehman, C. Xiong, R. Socher, and B. C. Wallace, "ERASER: A benchmark to evaluate rationalized NLP models," in *Proceedings of the 58th Annual Meeting of the Association for Computational Linguistics*, 2020, pp. 4443–4458.

[39] H. Jhamtani and P. Clark, "Learning to explain: Datasets and models for identifying valid reasoning chains in multihop question-answering," in *Proceedings of the 2020 Conference on Empirical Methods in Natural Language Processing*, 2020, p. 137–150.

[40] O. Tafjord, B. D. Mishra, and P. Clark, "Proofwriter: Generating implications, proofs, and abductive statements over natural language," in *Findings of the Association for Computational Linguistics: ACL-IJCNLP*, 2021, p. 3621–3634.

[41] C. Zhao, C. Xiong, J. Boyd-Graber, and H. Daumé III, "Multi-step reasoning over unstructured text with beam dense retrieval," in *Proceedings of the 2021 Conference of the North American Chapter of the Association for Computational Linguistics: Human Language Technologies*, 2021, pp. 4635–4641.

[42] B. Dalvi, P. Jansen, O. Tafjord, Z. Xie, H. Smith, L. Pipatanangkura, and P. Clark, "Explaining answers with entailment trees," in *Proceedings of the 2021 Conference on Empirical Methods in Natural Language Processing*, 2021, pp. 7358–7370.

[43] Y. Zhang, J. Yang, Y. Yuan, and A. C.-C. Yao, "Cumulative reasoning with large language models," in *ICLR 2024 Workshop on Bridging the Gap Between Practice and Theory in Deep Learning*, 2024. [Online]. Available: <https://openreview.net/forum?id=XAAAYyRxtIQ>

[44] V. Liévin, C. E. Hother, A. G. Motzfeldt, and O. Winther, "Can large language models reason about medical questions?" *Patterns*, vol. 5, no. 3, 2024.

[45] Y. Gao, D. Dligach, T. Miller, J. Caskey, B. Sharma, M. M. Churpek, and M. Afshar, "Dr. bench: Diagnostic reasoning benchmark for clinical natural language processing," *Journal of Biomedical Informatics*, vol. 138, p. 104286, 2023.

[46] L. Weed, *Medical Records, Medical Education, and Patient Care: The Problem-oriented Record as a Basic Tool*. Press of Case Western Reserve University, 1970.

[47] O. Bodenreider, "The unified medical language system (umls): integrating biomedical terminology," *Nucleic acids research*, vol. 32, no. suppl_1, pp. D267–D270, 2004.

[48] M. Zhang, *Criminal Law*, 5th ed. Beijing, China: Law Press China, 2016.



Junhao Chen received a B.S. degree in Applied Statistics from South China Normal University, China, in 2023. He is currently an M.Phil. student in Artificial Intelligence at The Hong Kong University of Science and Technology (Guangzhou) and an intern at the D3 Center, Osaka University, Japan. His research interests include explainable AI, large language models, and medical AI.



Jiuyang Chang MD, PhD, earned his doctorate from the Department of Cardiovascular Medicine, Graduate School of Medicine, Osaka University. He previously served as a Specially Appointed Researcher in Osaka University. Dr. Chang was awarded the JSPS (Japan Society for the Promotion of Science) Grant-in-Aid for Research Start-up and received the International Young Investigator Award (YIA) from the Japanese Circulation Society. He is currently a Physician in the Department of Cardiovascular Medicine at The First Affiliated Hospital of Dalian Medical University and is recognized as a Dalian High-Level Talent. Dr. Chang has been granted the Liaoning Provincial Natural Science Foundation Doctoral Research Start-up Fund. His research focuses on lipid metabolism and interdisciplinary research in medicine and engineering, with 14 SCI-indexed publications to his credit.



medical AI.

Bowen Wang received a B.S. and M.S. degree in Computer Science from Anhui University, China, in 2016 and in Medical Information from Osaka University, Japan, in 2020, respectively, and a Ph.D. degree in Computer Science from Osaka University, in 2023. He has received the best paper award in APAMI 2020 and is a member of IEEE. He is currently a specially-appointed assistant professor with the D3 center and WPI Prime, The University of Osaka, Japan. His research interests in computer vision, explainable AI, large language models, and



Yuta Nakashima (M'09) received the B.E. and M.E. degrees in communication engineering and the Ph.D. degree in engineering from Osaka University, Osaka, Japan, in 2006, 2008, and 2012, respectively. From 2012 to 2016, he was an Assistant Professor at the Nara Institute of Science and Technology. He is currently a Professor at SANKEN, department of Intelligent Media, The University of Osaka. He was a Visiting Scholar at the University of North Carolina at Charlotte in 2012 and at Carnegie Mellon University from 2015 to 2016. His research interests include computer vision and machine learning and their applications. His main research includes video content analysis using machine learning approaches. Prof. Nakashima is a member of ACM, IEICE, and IPSJ.